BABAR-CONF-08/018
SLAC-PUB-13334
arXiv:0807.4978 [hep-ex]

Measurement of $|V_{cb}|$ and the form-factor slope for $\overline{B} \to D\ell^-\bar{\nu}_\ell$ decays on the recoil of fully reconstructed B mesons

The *BABAR* Collaboration

August 19, 2008

Abstract

We present a measurement of the CKM matrix element $|V_{cb}|$ and the form-factor slope ρ^2 for $\overline{B} \to D\ell^-\bar{\nu}_\ell$ decays based on 417 fb^{-1} of data collected at the $\Upsilon(4S)$ resonance with the *BABAR* detector. The semileptonic decays are selected in $B\overline{B}$ events in which the hadronic decay of the second B meson is fully reconstructed. From the measured differential decay rate of the signal decay we determine $\mathcal{G}(1)|V_{cb}| = (43.0 \pm 1.9 \pm 1.4) \times 10^{-3}$, $\rho^2 = 1.20 \pm 0.09 \pm 0.04$, where $\mathcal{G}(1)$ is the hadronic form factor at the point of zero recoil. Using a lattice calculation for $\mathcal{G}(1)$ we extract $|V_{cb}| = (39.8 \pm 1.8 \pm 1.3 \pm 0.9) \times 10^{-3}$, where the stated errors refer to the statistical, systematic, and form factor uncertainties. We also present a measurement of the exclusive branching fractions, $\mathcal{B}(B^- \to D^0\ell^-\bar{\nu}_\ell) = (2.31 \pm 0.08 \pm 0.07)\%$ and $\mathcal{B}(\overline{B}^0 \to D^+\ell^-\bar{\nu}_\ell) = (2.23 \pm 0.11 \pm 0.08)\%$.

Submitted to the 34$^{\text{th}}$ International Conference on High-Energy Physics, ICHEP 08,
29 July—5 August 2008, Philadelphia, Pennsylvania.

Stanford Linear Accelerator Center, Stanford University, Stanford, CA 94309

Work supported in part by Department of Energy contract DE-AC02-76SF00515.

The *BABAR* Collaboration,

B. Aubert, M. Bona, Y. Karyotakis, J. P. Lees, V. Poireau, E. Prencipe, X. Prudent, V. Tisserand

Laboratoire de Physique des Particules, IN2P3/CNRS et Université de Savoie, F-74941 Annecy-Le-Vieux, France

J. Garra Tico, E. Grauges

Universitat de Barcelona, Facultat de Fisica, Departament ECM, E-08028 Barcelona, Spain

L. Lopez[ab], A. Palano[ab], M. Pappagallo[ab]

INFN Sezione di Bari[a]; Dipartmento di Fisica, Università di Bari[b], I-70126 Bari, Italy

G. Eigen, B. Stugu, L. Sun

University of Bergen, Institute of Physics, N-5007 Bergen, Norway

G. S. Abrams, M. Battaglia, D. N. Brown, R. N. Cahn, R. G. Jacobsen, L. T. Kerth, Yu. G. Kolomensky, G. Lynch, I. L. Osipenkov, M. T. Ronan,[1] K. Tackmann, T. Tanabe

Lawrence Berkeley National Laboratory and University of California, Berkeley, California 94720, USA

C. M. Hawkes, N. Soni, A. T. Watson

University of Birmingham, Birmingham, B15 2TT, United Kingdom

H. Koch, T. Schroeder

Ruhr Universität Bochum, Institut für Experimentalphysik 1, D-44780 Bochum, Germany

D. Walker

University of Bristol, Bristol BS8 1TL, United Kingdom

D. J. Asgeirsson, B. G. Fulsom, C. Hearty, T. S. Mattison, J. A. McKenna

University of British Columbia, Vancouver, British Columbia, Canada V6T 1Z1

M. Barrett, A. Khan

Brunel University, Uxbridge, Middlesex UB8 3PH, United Kingdom

V. E. Blinov, A. D. Bukin, A. R. Buzykaev, V. P. Druzhinin, V. B. Golubev, A. P. Onuchin, S. I. Serednyakov, Yu. I. Skovpen, E. P. Solodov, K. Yu. Todyshev

Budker Institute of Nuclear Physics, Novosibirsk 630090, Russia

M. Bondioli, S. Curry, I. Eschrich, D. Kirkby, A. J. Lankford, P. Lund, M. Mandelkern, E. C. Martin, D. P. Stoker

University of California at Irvine, Irvine, California 92697, USA

S. Abachi, C. Buchanan

University of California at Los Angeles, Los Angeles, California 90024, USA

J. W. Gary, F. Liu, O. Long, B. C. Shen,[1] G. M. Vitug, Z. Yasin, L. Zhang

University of California at Riverside, Riverside, California 92521, USA

[1]Deceased

V. Sharma

University of California at San Diego, La Jolla, California 92093, USA

C. Campagnari, T. M. Hong, D. Kovalskyi, M. A. Mazur, J. D. Richman

University of California at Santa Barbara, Santa Barbara, California 93106, USA

T. W. Beck, A. M. Eisner, C. J. Flacco, C. A. Heusch, J. Kroseberg, W. S. Lockman, A. J. Martinez, T. Schalk, B. A. Schumm, A. Seiden, M. G. Wilson, L. O. Winstrom

University of California at Santa Cruz, Institute for Particle Physics, Santa Cruz, California 95064, USA

C. H. Cheng, D. A. Doll, B. Echenard, F. Fang, D. G. Hitlin, I. Narsky, T. Piatenko, F. C. Porter

California Institute of Technology, Pasadena, California 91125, USA

R. Andreassen, G. Mancinelli, B. T. Meadows, K. Mishra, M. D. Sokoloff

University of Cincinnati, Cincinnati, Ohio 45221, USA

P. C. Bloom, W. T. Ford, A. Gaz, J. F. Hirschauer, M. Nagel, U. Nauenberg, J. G. Smith, K. A. Ulmer, S. R. Wagner

University of Colorado, Boulder, Colorado 80309, USA

R. Ayad,[2] A. Soffer,[3] W. H. Toki, R. J. Wilson

Colorado State University, Fort Collins, Colorado 80523, USA

D. D. Altenburg, E. Feltresi, A. Hauke, H. Jasper, M. Karbach, J. Merkel, A. Petzold, B. Spaan, K. Wacker

Technische Universität Dortmund, Fakultät Physik, D-44221 Dortmund, Germany

M. J. Kobel, W. F. Mader, R. Nogowski, K. R. Schubert, R. Schwierz, A. Volk

Technische Universität Dresden, Institut für Kern- und Teilchenphysik, D-01062 Dresden, Germany

D. Bernard, G. R. Bonneaud, E. Latour, M. Verderi

Laboratoire Leprince-Ringuet, CNRS/IN2P3, Ecole Polytechnique, F-91128 Palaiseau, France

P. J. Clark, S. Playfer, J. E. Watson

University of Edinburgh, Edinburgh EH9 3JZ, United Kingdom

M. Andreotti[ab], D. Bettoni[a], C. Bozzi[a], R. Calabrese[ab], A. Cecchi[ab], G. Cibinetto[ab], P. Franchini[ab], E. Luppi[ab], M. Negrini[ab], A. Petrella[ab], L. Piemontese[a], V. Santoro[ab]

INFN Sezione di Ferrara[a]; Dipartimento di Fisica, Università di Ferrara[b], I-44100 Ferrara, Italy

R. Baldini-Ferroli, A. Calcaterra, R. de Sangro, G. Finocchiaro, S. Pacetti, P. Patteri, I. M. Peruzzi,[4] M. Piccolo, M. Rama, A. Zallo

INFN Laboratori Nazionali di Frascati, I-00044 Frascati, Italy

A. Buzzo[a], R. Contri[ab], M. Lo Vetere[ab], M. M. Macri[a], M. R. Monge[ab], S. Passaggio[a], C. Patrignani[ab], E. Robutti[a], A. Santroni[ab], S. Tosi[ab]

INFN Sezione di Genova[a]; Dipartimento di Fisica, Università di Genova[b], I-16146 Genova, Italy

[2]Now at Temple University, Philadelphia, Pennsylvania 19122, USA
[3]Now at Tel Aviv University, Tel Aviv, 69978, Israel
[4]Also with Università di Perugia, Dipartimento di Fisica, Perugia, Italy

K. S. Chaisanguanthum, M. Morii
Harvard University, Cambridge, Massachusetts 02138, USA

A. Adametz, J. Marks, S. Schenk, U. Uwer
Universität Heidelberg, Physikalisches Institut, Philosophenweg 12, D-69120 Heidelberg, Germany

V. Klose, H. M. Lacker
Humboldt-Universität zu Berlin, Institut für Physik, Newtonstr. 15, D-12489 Berlin, Germany

D. J. Bard, P. D. Dauncey, J. A. Nash, M. Tibbetts
Imperial College London, London, SW7 2AZ, United Kingdom

P. K. Behera, X. Chai, M. J. Charles, U. Mallik
University of Iowa, Iowa City, Iowa 52242, USA

J. Cochran, H. B. Crawley, L. Dong, W. T. Meyer, S. Prell, E. I. Rosenberg, A. E. Rubin
Iowa State University, Ames, Iowa 50011-3160, USA

Y. Y. Gao, A. V. Gritsan, Z. J. Guo, C. K. Lae
Johns Hopkins University, Baltimore, Maryland 21218, USA

N. Arnaud, J. Béquilleux, A. D'Orazio, M. Davier, J. Firmino da Costa, G. Grosdidier, A. Höcker, V. Lepeltier, F. Le Diberder, A. M. Lutz, S. Pruvot, P. Roudeau, M. H. Schune, J. Serrano, V. Sordini,[5] A. Stocchi, G. Wormser
Laboratoire de l'Accélérateur Linéaire, IN2P3/CNRS et Université Paris-Sud 11, Centre Scientifique d'Orsay, B. P. 34, F-91898 Orsay Cedex, France

D. J. Lange, D. M. Wright
Lawrence Livermore National Laboratory, Livermore, California 94550, USA

I. Bingham, J. P. Burke, C. A. Chavez, J. R. Fry, E. Gabathuler, R. Gamet, D. E. Hutchcroft, D. J. Payne, C. Touramanis
University of Liverpool, Liverpool L69 7ZE, United Kingdom

A. J. Bevan, C. K. Clarke, K. A. George, F. Di Lodovico, R. Sacco, M. Sigamani
Queen Mary, University of London, London, E1 4NS, United Kingdom

G. Cowan, H. U. Flaecher, D. A. Hopkins, S. Paramesvaran, F. Salvatore, A. C. Wren
University of London, Royal Holloway and Bedford New College, Egham, Surrey TW20 0EX, United Kingdom

D. N. Brown, C. L. Davis
University of Louisville, Louisville, Kentucky 40292, USA

A. G. Denig M. Fritsch, W. Gradl, G. Schott
Johannes Gutenberg-Universität Mainz, Institut für Kernphysik, D-55099 Mainz, Germany

[5]Also with Università di Roma La Sapienza, I-00185 Roma, Italy

K. E. Alwyn, D. Bailey, R. J. Barlow, Y. M. Chia, C. L. Edgar, G. Jackson, G. D. Lafferty, T. J. West, J. I. Yi
University of Manchester, Manchester M13 9PL, United Kingdom

J. Anderson, C. Chen, A. Jawahery, D. A. Roberts, G. Simi, J. M. Tuggle
University of Maryland, College Park, Maryland 20742, USA

C. Dallapiccola, X. Li, E. Salvati, S. Saremi
University of Massachusetts, Amherst, Massachusetts 01003, USA

R. Cowan, D. Dujmic, P. H. Fisher, G. Sciolla, M. Spitznagel, F. Taylor, R. K. Yamamoto, M. Zhao
Massachusetts Institute of Technology, Laboratory for Nuclear Science, Cambridge, Massachusetts 02139, USA

P. M. Patel, S. H. Robertson
McGill University, Montréal, Québec, Canada H3A 2T8

A. Lazzaro[ab], V. Lombardo[a], F. Palombo[ab]
INFN Sezione di Milano[a]; Dipartimento di Fisica, Università di Milano[b], I-20133 Milano, Italy

J. M. Bauer, L. Cremaldi R. Godang,[6] R. Kroeger, D. A. Sanders, D. J. Summers, H. W. Zhao
University of Mississippi, University, Mississippi 38677, USA

M. Simard, P. Taras, F. B. Viaud
Université de Montréal, Physique des Particules, Montréal, Québec, Canada H3C 3J7

H. Nicholson
Mount Holyoke College, South Hadley, Massachusetts 01075, USA

G. De Nardo[ab], L. Lista[a], D. Monorchio[ab], G. Onorato[ab], C. Sciacca[ab]
INFN Sezione di Napoli[a]; Dipartimento di Scienze Fisiche, Università di Napoli Federico II[b], I-80126 Napoli, Italy

G. Raven, H. L. Snoek
NIKHEF, National Institute for Nuclear Physics and High Energy Physics, NL-1009 DB Amsterdam, The Netherlands

C. P. Jessop, K. J. Knoepfel, J. M. LoSecco, W. F. Wang
University of Notre Dame, Notre Dame, Indiana 46556, USA

G. Benelli, L. A. Corwin, K. Honscheid, H. Kagan, R. Kass, J. P. Morris, A. M. Rahimi, J. J. Regensburger, S. J. Sekula, Q. K. Wong
Ohio State University, Columbus, Ohio 43210, USA

N. L. Blount, J. Brau, R. Frey, O. Igonkina, J. A. Kolb, M. Lu, R. Rahmat, N. B. Sinev, D. Strom, J. Strube, E. Torrence
University of Oregon, Eugene, Oregon 97403, USA

[6]Now at University of South Alabama, Mobile, Alabama 36688, USA

G. Castelli[ab], N. Gagliardi[ab], M. Margoni[ab], M. Morandin[a], M. Posocco[a], M. Rotondo[a], F. Simonetto[ab], R. Stroili[ab], C. Voci[ab]

INFN Sezione di Padova[a]; Dipartimento di Fisica, Università di Padova[b], I-35131 Padova, Italy

P. del Amo Sanchez, E. Ben-Haim, H. Briand, G. Calderini, J. Chauveau, P. David, L. Del Buono, O. Hamon, Ph. Leruste, J. Ocariz, A. Perez, J. Prendki, S. Sitt

Laboratoire de Physique Nucléaire et de Hautes Energies, IN2P3/CNRS, Université Pierre et Marie Curie-Paris6, Université Denis Diderot-Paris7, F-75252 Paris, France

L. Gladney

University of Pennsylvania, Philadelphia, Pennsylvania 19104, USA

M. Biasini[ab], R. Covarelli[ab], E. Manoni[ab],

INFN Sezione di Perugia[a]; Dipartimento di Fisica, Università di Perugia[b], I-06100 Perugia, Italy

C. Angelini[ab], G. Batignani[ab], S. Bettarini[ab], M. Carpinelli[ab],[7] A. Cervelli[ab], F. Forti[ab], M. A. Giorgi[ab], A. Lusiani[ac], G. Marchiori[ab], M. Morganti[ab], N. Neri[ab], E. Paoloni[ab], G. Rizzo[ab], J. J. Walsh[a]

INFN Sezione di Pisa[a]; Dipartimento di Fisica, Università di Pisa[b]; Scuola Normale Superiore di Pisa[c], I-56127 Pisa, Italy

D. Lopes Pegna, C. Lu, J. Olsen, A. J. S. Smith, A. V. Telnov

Princeton University, Princeton, New Jersey 08544, USA

F. Anulli[a], E. Baracchini[ab], G. Cavoto[a], D. del Re[ab], E. Di Marco[ab], R. Faccini[ab], F. Ferrarotto[a], F. Ferroni[ab], M. Gaspero[ab], P. D. Jackson[a], L. Li Gioi[a], M. A. Mazzoni[a], S. Morganti[a], G. Piredda[a], F. Polci[ab], F. Renga[ab], C. Voena[a]

INFN Sezione di Roma[a]; Dipartimento di Fisica, Università di Roma La Sapienza[b], I-00185 Roma, Italy

M. Ebert, T. Hartmann, H. Schröder, R. Waldi

Universität Rostock, D-18051 Rostock, Germany

T. Adye, B. Franek, E. O. Olaiya, F. F. Wilson

Rutherford Appleton Laboratory, Chilton, Didcot, Oxon, OX11 0QX, United Kingdom

S. Emery, M. Escalier, L. Esteve, S. F. Ganzhur, G. Hamel de Monchenault, W. Kozanecki, G. Vasseur, Ch. Yèche, M. Zito

CEA, Irfu, SPP, Centre de Saclay, F-91191 Gif-sur-Yvette, France

X. R. Chen, H. Liu, W. Park, M. V. Purohit, R. M. White, J. R. Wilson

University of South Carolina, Columbia, South Carolina 29208, USA

M. T. Allen, D. Aston, R. Bartoldus, P. Bechtle, J. F. Benitez, R. Cenci, J. P. Coleman, M. R. Convery, J. C. Dingfelder, J. Dorfan, G. P. Dubois-Felsmann, W. Dunwoodie, R. C. Field, A. M. Gabareen, S. J. Gowdy, M. T. Graham, P. Grenier, C. Hast, W. R. Innes, J. Kaminski, M. H. Kelsey, H. Kim, P. Kim, M. L. Kocian, D. W. G. S. Leith, S. Li, B. Lindquist, S. Luitz, V. Luth, H. L. Lynch, D. B. MacFarlane, H. Marsiske, R. Messner, D. R. Muller, H. Neal, S. Nelson, C. P. O'Grady, I. Ofte, A. Perazzo, M. Perl, B. N. Ratcliff, A. Roodman, A. A. Salnikov, R. H. Schindler, J. Schwiening, A. Snyder, D. Su, M. K. Sullivan, K. Suzuki, S. K. Swain, J. M. Thompson, J. Va'vra, A. P. Wagner, M. Weaver, C. A. West, W. J. Wisniewski, M. Wittgen, D. H. Wright, H. W. Wulsin, A. K. Yarritu, K. Yi, C. C. Young, V. Ziegler

Stanford Linear Accelerator Center, Stanford, California 94309, USA

[7]Also with Università di Sassari, Sassari, Italy

P. R. Burchat, A. J. Edwards, S. A. Majewski, T. S. Miyashita, B. A. Petersen, L. Wilden
Stanford University, Stanford, California 94305-4060, USA

S. Ahmed, M. S. Alam, J. A. Ernst, B. Pan, M. A. Saeed, S. B. Zain
State University of New York, Albany, New York 12222, USA

S. M. Spanier, B. J. Wogsland
University of Tennessee, Knoxville, Tennessee 37996, USA

R. Eckmann, J. L. Ritchie, A. M. Ruland, C. J. Schilling, R. F. Schwitters
University of Texas at Austin, Austin, Texas 78712, USA

B. W. Drummond, J. M. Izen, X. C. Lou
University of Texas at Dallas, Richardson, Texas 75083, USA

F. Bianchi[ab], D. Gamba[ab], M. Pelliccioni[ab]
INFN Sezione di Torino[a]; Dipartimento di Fisica Sperimentale, Università di Torino[b], I-10125 Torino, Italy

M. Bomben[ab], L. Bosisio[ab], C. Cartaro[ab], G. Della Ricca[ab], L. Lanceri[ab], L. Vitale[ab]
INFN Sezione di Trieste[a]; Dipartimento di Fisica, Università di Trieste[b], I-34127 Trieste, Italy

V. Azzolini, N. Lopez-March, F. Martinez-Vidal, D. A. Milanes, A. Oyanguren
IFIC, Universitat de Valencia-CSIC, E-46071 Valencia, Spain

J. Albert, Sw. Banerjee, B. Bhuyan, H. H. F. Choi, K. Hamano, R. Kowalewski, M. J. Lewczuk, I. M. Nugent, J. M. Roney, R. J. Sobie
University of Victoria, Victoria, British Columbia, Canada V8W 3P6

T. J. Gershon, P. F. Harrison, J. Ilic, T. E. Latham, G. B. Mohanty
Department of Physics, University of Warwick, Coventry CV4 7AL, United Kingdom

H. R. Band, X. Chen, S. Dasu, K. T. Flood, Y. Pan, M. Pierini, R. Prepost, C. O. Vuosalo, S. L. Wu
University of Wisconsin, Madison, Wisconsin 53706, USA

1 Introduction

The study of the semileptonic decay $\overline{B} \to D\ell^-\bar{\nu}_\ell$ is interesting in many aspects. In the standard model, the rate of this weak decay is proportional to the square of the Cabibbo-Kobayashi-Maskawa (CKM) [1] matrix element $|V_{cb}|$, which is a measure of the weak coupling of the b to the c quark.

The decay rate is also proportional to the square of the hadronic matrix element, which accounts for the effects of strong interactions in the $\overline{B} \to D$ transition. In the limit of very small masses of the lepton, $\ell = e$ or μ, their effect can be parameterized by a single form factor $\mathcal{G}(w)$, where the variable w (see below) is linearly related to the momentum transfer squared q^2 of the B meson to the D meson.

The extraction of $|V_{cb}|$ relies on the measurement of differential decay rates of semileptonic B decays. The precise determination requires corrections to the prediction for the normalization at $w = 1$ in the context of Heavy Quark Symmetry [2], as well as a measurement of the variation of the form factors near the kinematic limit, $w = 1$, where the decay rate goes to zero as the phase space vanishes.

Measurements of $|V_{cb}|$ based on studies of the differential decay rate for $\overline{B} \to D\ell^-\bar{\nu}_\ell$ decays have previously been reported by Belle [3], CLEO [4] and ALEPH [5].

In this paper, we present preliminary measurements of the differential decay rates, separately for $\overline{B}^0 \to D^+\ell^-\bar{\nu}_\ell$ and $B^- \to D^0\ell^-\bar{\nu}_\ell$ [6]. Semileptonic decays are selected in $B\overline{B}$ events in which an hadronic decay of the second B meson is also fully reconstructed. This leads to a very clean sample of events and also provides a precise measurement for the variable q^2, and thereby w. The measurement of the total branching fractions and the extraction of $|V_{cb}|$ requires an absolute normalization. We use a sample of inclusive semileptonic decays, $\overline{B} \to X\ell^-\bar{\nu}_\ell$, where only the charged lepton is reconstructed. This choice reduces the uncertainty of the normalization, because the lepton is also selected from a sample tagged by hadronic decays of the second B meson.

2 Parameterization of the Decay Rate

In the limit of small lepton masses the partial decay rate for $\overline{B} \to D\ell^-\bar{\nu}_\ell$ can be expressed in terms of a single form factor, $\mathcal{G}(w)$,

$$\frac{\mathrm{d}\Gamma(B \to D\ell\nu)}{\mathrm{d}w} \quad = \quad \frac{G_F^2}{48\pi^3\hbar} M_D^3 (M_B + M_D)^2 \; (w^2 - 1)^{3/2} \; \mid V_{cb} \mid^2 \; \mathcal{G}^2(w), \tag{1}$$

where G_F is the Fermi coupling constant, and M_B and M_D are the masses of the B and D mesons. The variable w denotes the product of the B and D meson four-velocities V_B and V_D,

$$w = V_B \cdot V_D = \frac{(M_B^2 + M_D^2 - q^2)}{(2M_B M_D)}, \tag{2}$$

where $q^2 \equiv (p_B - p_D)^2$, and p_B and p_D refer to the four-momenta of the B and D mesons. Its lower limit, $w = 1$, corresponds to zero recoil of the D meson, *i.e.* the maximum q^2. The upper limit, $w = 1.59$, corresponds to $q^2 = 0$ and the maximum D momentum. Since the B momentum is known from the fully reconstructed B_{tag} in the same event, w can be reconstructed with good precision, namely to ~ 0.01, which corresponds to about 2% of the full kinematic range.

In the limit of infinite quark masses $\mathcal{G}(w)$ coincides with the Isgur-Wise function [7]. This function is normalized to unity at zero recoil. Corrections to this prediction have recently been calculated with improved precision, based on unquenched lattice QCD [8], specifically $\mathcal{G}(1) =$

$1.074 \pm 0.018 \pm 0.016$. Thus $|V_{cb}|$ can be extracted by extrapolating the differential decay rates to $w = 1$. To reduce the uncertainties associated with this extrapolation, constraints on the shape of the form factors are highly desirable. Several functional forms have been proposed [9]. We adopt the parameterization based on analyticity and positivity of the QCD functions which describe the local currents [10]. Specifically, $\mathcal{G}(w)$ is expressed as a polynomial in z,

$$\mathcal{G}(w) \;=\; \mathcal{G}(1)\left[1 - 8\rho^2 z + (51\rho^2 - 10)z^2 - (252\rho^2 - 84)z^3\right], \tag{3}$$

where the variable z is defined as $z = (\sqrt{w+1} - \sqrt{2})/(\sqrt{w+1} + \sqrt{2})$. This formulation expresses the non-linear dependence of the form factor on w in terms of a single shape parameter, ρ^2.

3 The *BABAR* Detector and Dataset

This analysis is based on 417 fb^{-1} of data collected at the $\Upsilon(4S)$ resonance with the *BABAR* detector at the PEP-II storage rings. The corresponding number of produced $B\overline{B}$ pairs is 460 million. In addition, 40 fb^{-1} of data, recorded at a center-of-mass energy 40 MeV below the $\Upsilon(4S)$ resonance, are used to study background from $e^+e^- \to f\bar{f}$ ($f = u, d, s, c, \tau$) events (continuum production). The *BABAR* detector is described in detail elsewhere [11]. Charged-particle trajectories are measured by a 5-layer double-sided silicon vertex tracker and a 40-layer drift chamber, both operating in a 1.5-T magnetic field. Charged-particle identification is provided by the average energy loss ($\mathrm{d}E/\mathrm{d}x$) in the tracking devices and by an internally reflecting ring-imaging Cherenkov detector. Photons are detected by a CsI(Tl) electromagnetic calorimeter (EMC). Muons are identified by the instrumented magnetic-flux return. A detailed GEANT4-based Monte Carlo (MC) simulation [12] of $B\overline{B}$ and continuum events has been used to study the detector response, its acceptance, and to test the analysis procedure. The simulation models the signal $\overline{B} \to D\ell^-\bar{\nu}_\ell$ decays using the ISGW2 model [13], and these are then reweighted to the HQET model described above. Other semileptonic decays that contribute to background are simulated as follows: for $\overline{B} \to D^*\ell^-\bar{\nu}_\ell$ decays we use form factor parametrizations based on Heavy Quark Effective Theory (HQET) with parameters determined by the *BABAR* collaboration [14], for $\overline{B} \to D^{**}(\to D^{(*)}\pi)\ell^-\bar{\nu}_\ell$ decays we use the ISGW2 model [13], and for decay involving non-resonant charm states, $\overline{B} \to D^{(*)}\pi\ell^-\bar{\nu}_\ell$, we adopt the prescription of the Goity-Roberts model [15]. The MC simulation includes radiative effects such as bremsstrahlung in the detector material. QED final state radiation is modeled by PHOTOS [16], and decays with radiative photons are included in the signal sample.

4 Event Selection

We select semileptonic B meson decays in events containing a fully reconstructed B meson (B_{tag}), which allows us to constrain the kinematics, to reduce the combinatorial background, and to determine the charge and flavor of the signal B.

The analysis exploits the presence of two charmed mesons in the final state: one is used for the exclusive reconstruction of the B_{tag}, and the other one for the reconstruction of the semileptonic B decay.

We first reconstruct the semileptonic B decay, selecting a lepton with momentum in the center-of-mass (CM) frame p^*_ℓ higher than 0.6 GeV/c. Electrons from photon conversion and π^0 Dalitz decays are removed using a dedicated algorithm, which performs the reconstruction of vertices between tracks of opposite charge whose invariant mass is compatible with a photon conversion or a π^0 Dalitz decay. Candidate D^0 mesons, with the correct charge correlation with the lepton, are reconstructed in the $K^-\pi^+$, $K^-\pi^+\pi^0$, $K^-\pi^+\pi^+\pi^-$, $K^0_S\pi^+\pi^-$, $K^0_S\pi^+\pi^-\pi^0$, $K^0_S\pi^0$, K^+K^-, $\pi^+\pi^-$, and $K^0_SK^0_S$ channels, and D^+ mesons in the $K^-\pi^+\pi^+$, $K^-\pi^+\pi^+\pi^0$, $K^0_S\pi^+$, $K^0_S\pi^+\pi^0$, $K^+K^-\pi^+$, $K^0_SK^+$, and $K^0_S\pi^+\pi^+\pi^-$ channels. D candidates are selected within 2σ of the D mass, with σ typically around 8 MeV/c^2. In events with multiple $\overline{B} \to D\ell^-\bar{\nu}_\ell$ candidates, the candidate with the largest D-ℓ^- vertex fit probability is selected.

We reconstruct $B_{\rm tag}$ decays of the type $\overline{B} \to D^{(*)}Y$, where Y represents a collection of hadrons with a total charge of ±1, composed of $n_1\pi^\pm + n_2K^\pm + n_3K^0_S + n_4\pi^0$, where $n_1 + n_2 \leq 5$, $n_3 \leq 2$, and $n_4 \leq 2$. Using $D^0(D^+)$ and $D^{*0}(D^{*+})$ as seeds for $B^-(\overline{B}^0)$ decays, we reconstruct about 1000 decay modes.

The kinematic consistency of a $B_{\rm tag}$ candidate with a B meson is checked using two variables: the beam-energy substituted mass $m_{ES} = \sqrt{s/4 - \vec{p}_B^{\,2}}$, and the energy difference $\Delta E = E_B - \sqrt{s}/2$. Here $\sqrt{s}$ refers to the total CM energy, and $\vec{p}_B$ and E_B denote the momentum and energy of the $B_{\rm tag}$ candidate in the CM frame. For correctly identified $B_{\rm tag}$ decays, the m_{ES} distribution peaks at the B meson mass, while ΔE is consistent with zero. We select a $B_{\rm tag}$ candidate in the signal region defined as 5.27 GeV/c^2 $< m_{ES} <$ 5.29 GeV/c^2, excluding $B_{\rm tag}$ candidates with daughter particles in common with the charm meson or with the lepton from the semileptonic B decay. In the case of multiple $B_{\rm tag}$ candidates, we select the one with the smallest $|\Delta E|$ value. For charged B events, the $B_{\rm tag}$ and the $D\ell^-$ candidates are required to have the correct charge-flavor correlation. We do not apply any correction to account for $B^0 - \overline{B}^0$ mixing effects, because they are found to be negligible. Cross-feed effects, *i.e.* $B^-_{\rm tag}(\overline{B}^0_{\rm tag})$ candidates erroneously reconstructed as a neutral (charged) B, are subtracted using the MC simulation.

Semileptonic B decays are identified by the missing mass squared, defined as:

$$m^2_{\rm miss} = [p(\Upsilon(4S)) - p(B_{\rm tag}) - p(D) - p(\ell)]^2 \qquad (4)$$

in terms of the particle four-momenta. For correctly reconstructed signal events, the only missing particle is the neutrino, and the $m^2_{\rm miss}$ peaks at zero. Other semileptonic B decays, like $\overline{B} \to D^*\ell^-\bar{\nu}_\ell$ and $\overline{B} \to D^{**}\ell^-\bar{\nu}_\ell$, where one particle is not reconstructed (feed-down), spread to higher values of $m^2_{\rm miss}$. The use of the full-reconstruction technique results in a $m^2_{\rm miss}$ resolution of 0.04 GeV$^2/c^4$, an order of magnitude better than achieved in non-tagged analyses [17].

5 Measurement of $|V_{cb}|$ and ρ^2

We measure $|V_{cb}|$ and the form-factor slope ρ^2 by a fit to the w distribution for $\overline{B} \to D\ell^-\bar{\nu}_\ell$ decays.

Data and Monte Carlo events are collected in ten equal-size w bins. The few events that have $w < 1.0$ or $w > 1.59$ due to resolution effects, are collected in the first bin and the last bin, respectively.

To obtain the semileptonic $\overline{B} \to D\ell^-\bar{\nu}_\ell$ signal yield in the different w intervals, we perform a one-dimensional extended binned maximum likelihood fit to the $m^2_{\rm miss}$ distributions, based on a method developed by R. Barlow and C. Beeston [18]. The fitted data samples are assumed to contain four different types of events:

- signal $\overline{B} \to D\ell^-\bar{\nu}_\ell$,
- feed-down semileptonic B decays,

- $B\overline{B}$ and continuum background,
- fake lepton events.

We use the Monte Carlo predictions for the different semileptonic B decay $m^2_{\rm miss}$ distributions to obtain the Probability Density Functions (PDFs) to fit the data distributions. The feed-down contributions are allowed to float independently in the different w intervals. We use the off-peak data to provide the continuum background normalization, while the $B\overline{B}$ normalization is taken from the MC. The shape of the continuum background predicted by the MC simulation is consistent with the one obtained from the off-peak data.

The $m^2_{\rm miss}$ distributions for two different w intervals are compared with the results of the fits in Fig. 1.

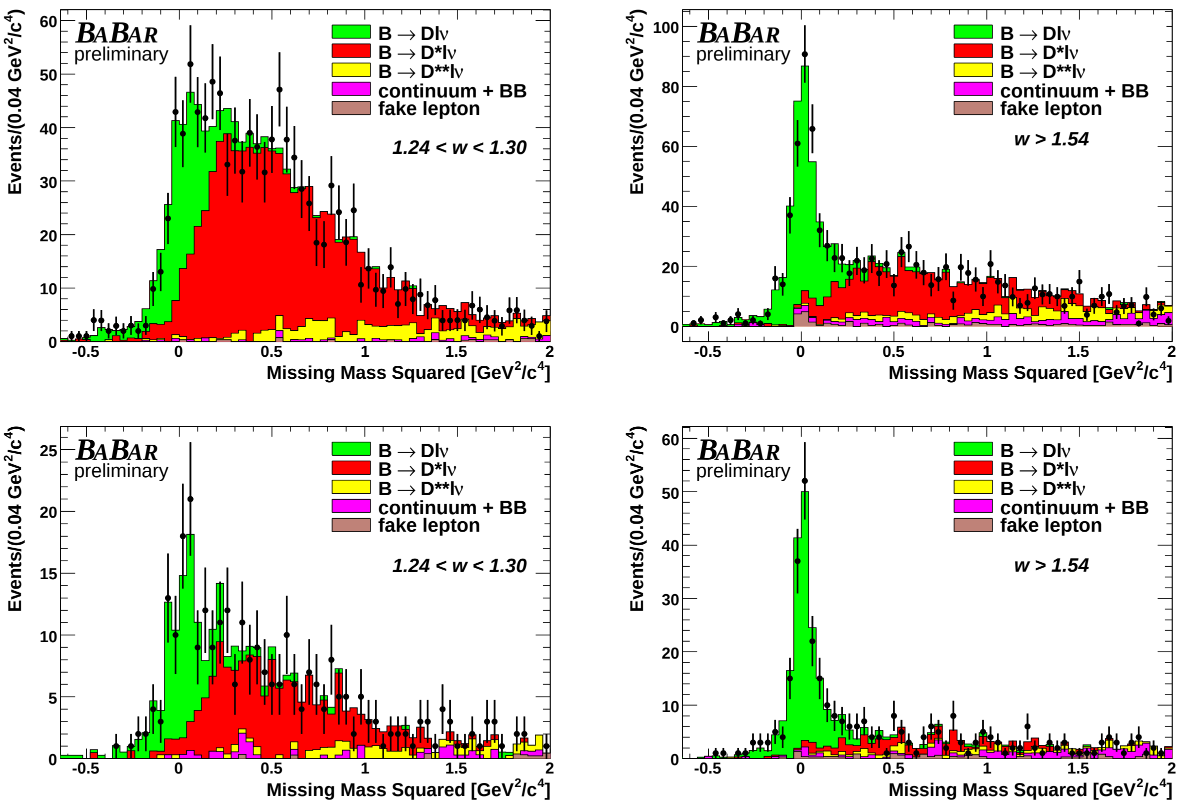

Figure 1: Fit to the $m^2_{\rm miss}$ distribution, in two different w intervals, for $B^- \to D^0\ell^-\bar{\nu}_\ell$ (top row), $\overline{B}^0 \to D^+\ell^-\bar{\nu}_\ell$ (bottom row): the data (points with error bars) are compared to the results of the overall fit (sum of the solid histograms). The PDFs for the different fit components are stacked and shown in different colors.

The signal yields in bins of w are displayed in Fig. 2. A χ^2 fit is performed on the w distributions comparing the number of events observed in each interval to the MC signal prediction. The signal prediction is obtained by properly weighting each MC event. The χ^2 is defined as:

$$\chi^2 = \sum_{i=1}^{10} \frac{(N^i_{\text{data}} - \sum_{j=1}^{N^i_{\text{MC}}} W^i_j)^2}{(\sigma^i_{\text{data}})^2 + \sum_{j=1}^{N^i_{\text{MC}}} {W^i_j}^2}, \tag{5}$$

where the index i runs over the ten w bins; N^i_{data} is the observed number of signal events found in the i^{th} bin and the σ^i_{data} the corresponding error. The expected signal yields are calculated at each step of the minimization from the reweighted sum of N^i_{MC} simulated events. The Monte Carlo is corrected event by event for all known differences in tracking, cluster reconstruction and particle identification determined from data control samples. The weight for each Monte Carlo event is computed as the product of two terms $W^i_j = W^{\mathcal{L}} \times W^{i,\text{theo}}_j$ where

- $W^{\mathcal{L}}$ is an overall fixed scale factor that accounts for the relative luminosity of data and signal Monte Carlo events; this is obtained, as described below, by normalizing to the inclusive yield of $\overline{B} \to X\ell^-\bar{\nu}_\ell$ events, corrected for its reconstruction efficiency, and scaled to the absolute $\overline{B} \to X\ell^-\bar{\nu}_\ell$ branching fraction [19].
- $W^{i,\text{theo}}_j = f^{\text{theo}}(w^i_j; \rho^2, \mathcal{G}(1)|V_{cb}|)/f_{\text{MC}}(w^i_j; \rho^2_{\text{MC}}, \mathcal{G}(1)|V_{cb}|_{\text{MC}})$ is the term that describes the differential decay rate. It depends on $\mathcal{G}(1)|V_{cb}|$ and ρ^2, and varies at each step of the minimization.

Here w^i_j is the true w of the MC event j, reconstructed in the i-bin. The function f^{theo} corresponds to the expressions in Eq. 1 and 3, while f_{MC} is the function used to generate $\overline{B} \to D\ell^-\bar{\nu}_\ell$ Monte Carlo events [8].

We first fit separately the w distributions for the charged and neutral $\overline{B} \to D\ell^-\bar{\nu}_\ell$ samples; we also perform a combined fit for $\overline{B} \to D\ell^-\bar{\nu}_\ell$, assuming that $f_{00} + f_{+-} = 1$, *i.e.* that B^+B^- and $B^0\overline{B}^0$ together saturate the $\Upsilon(4S)$ decays. The value of the branching ratio is then computed by integrating the differential expression in Eq. 1.

In Fig. 2 we show the comparison between the data and the fit results separately for $B^- \to D^0\ell^-\bar{\nu}_\ell$ and $\overline{B}^0 \to D^+\ell^-\bar{\nu}_\ell$. The corresponding distributions for the combined fit are shown in Fig. 3. The measured values of $\mathcal{G}(1)|V_{cb}|$ and ρ^2, with the corresponding correlation ρ_{corr} obtained from the fit, are reported in Table 1 and shown in Fig. 4.

For the measurement of $\mathcal{G}(1)|V_{cb}|$, in order to reduce the systematic uncertainty, we use as normalization a sample of inclusive $\overline{B} \to X\ell^-\bar{\nu}_\ell$ decays. These events are selected by identifying a charged lepton with CM momentum greater than 0.6 GeV/c. In the case of multiple B_{tag} candidates, we select the one reconstructed in the decay channel with the highest purity, defined as the fraction of signal events in the m_{ES} signal region. We require the lepton and the B_{tag} to have the correct charge correlation and the lepton track to not be used to reconstruct the B_{tag} candidate. Background components peaking in the m_{ES} signal region include cascade B meson decays (i.e. the lepton does not come directly from the B) and hadronic decays where one of the hadrons is misidentified as a lepton. These backgrounds are subtracted by using the corresponding simulated Monte Carlo distributions. The cascade-B meson decays (17.6% and 19.0% of the total m_{ES} distribution for charged and neutral B, respectively) are reweighted to account for differences between the branching fractions used in our Monte Carlo simulation and the latest experimental measurements [20]. The total yield for the inclusive $\overline{B} \to X\ell^-\bar{\nu}_\ell$ decays is obtained from a maximum-likelihood fit to the m_{ES} distribution of the B_{tag} candidates, using

[8] Corresponding to the CLN parameterization [10], with $\rho^2 = 1.17$.

Table 1: Fit results for each sample. In the last column we report the results for the $\overline{B}^0$ and B^- combined fit, where the branching fraction refers to $\overline{B}^0$ decays. We also report the signal yields and the reconstruction efficiencies, integrated over the full w range. Only the statistical errors are reported here.

	$B^- \to D^0\ell^-\bar{\nu}_\ell$	$\overline{B}^0 \to D^+\ell^-\bar{\nu}_\ell$	$\overline{B} \to D\ell^-\bar{\nu}_\ell$
$\mathcal{G}(1)\lvert V_{cb}\rvert \cdot 10^3$	41.7± 2.1	45.6± 3.3	43.0± 1.9
ρ^2	1.14± 0.11	1.29± 0.14	1.20± 0.09
$\rho_{\rm corr}$	0.943	0.950	0.952
χ^2/ndf	3.4/8	5.6/8	9.9/18
Signal Yield	2147 ± 69	1108 ± 45	-
Recon. efficiency	$(1.99 \pm 0.02) \cdot 10^{-4}$	$(1.09 \pm 0.02) \cdot 10^{-4}$	-
$\mathcal{B}$	(2.31± 0.08)%	(2.23± 0.11)%	(2.17± 0.06)%

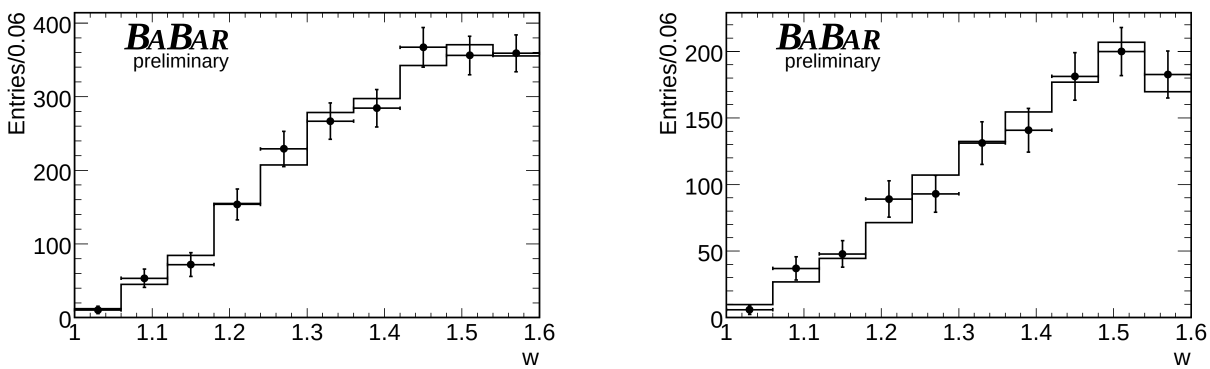

Figure 2: The w distribution for $\overline{B} \to D\ell^-\bar{\nu}_\ell$ events. Left: $B^- \to D^0\ell^-\bar{\nu}_\ell$, right: $\overline{B}^0 \to D^+\ell^-\bar{\nu}_\ell$. The data (points with error bars) are compared to the results of the overall fit (solid histogram).

an ARGUS function [21] for the description of the combinatorial $B\overline{B}$ and continuum background, and a Crystal Ball function [22] for the signal. A broad peaking component is observed in the m_{ES} signal region and is included in the signal definition. This is due to real $\overline{B} \to X\ell^-\bar{\nu}_\ell$ decays for which, in the $B_{\rm tag}$ reconstruction, neutral particles are not reconstructed or are interchanged with the semileptonic decays (e.g. a γ from radiative D^{*0} decay which belongs to the D^{*0} seed in the $B_{\rm tag}$ decay chain and is instead associated with a $B^- \to D^{*0}(D^0\gamma)\ell^-\bar{\nu}_\ell$ decay). This broad peaking component is modeled with additional Crystal Ball and ARGUS functions, whose parameters are fixed to the Monte Carlo prediction, except for the Crystal Ball mean value. Fig. 5 shows the m_{ES} distribution for the $B_{\rm tag}$ candidates in the $B^- \to X\ell^-\bar{\nu}_\ell$ and $\overline{B}^0 \to X\ell^-\bar{\nu}_\ell$ samples. The fit yields 198,897 ± 1,578 signal events in the $B^- \to X\ell^-\bar{\nu}_\ell$ sample and 116,330 ± 1,088 signal events in the $\overline{B}^0 \to X\ell^-\bar{\nu}_\ell$ sample. The corresponding reconstruction efficiencies, including the $B_{\rm tag}$ reconstruction, are 0.39% and 0.25%, respectively.

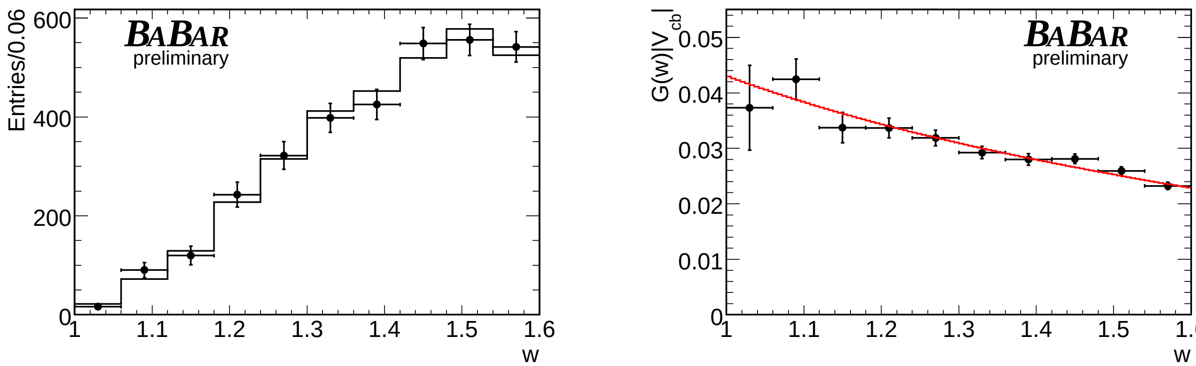

Figure 3: Left: w distribution obtained summing together $B^- \to D^0\ell^-\bar{\nu}_\ell$ and $\overline{B}^0 \to D^+\ell^-\bar{\nu}_\ell$ yields. The data (points with error bars) are compared to the results of the overall fit (solid histogram). Right: $\mathcal{G}(w)|V_{cb}|$ distribution unfolded for the reconstruction efficiency, with the fit result superimposed. These plots are not corrected for the smearing in w.

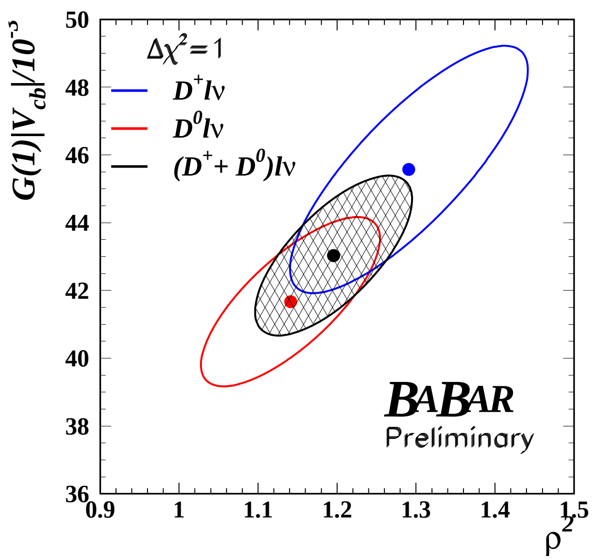

Figure 4: (left) $\Delta\chi^2 = 1$ ellipses in the $\mathcal{G}(1)|V_{cb}|$ versus ρ^2 plane for the $B^- \to D^0\ell^-\bar{\nu}_\ell$ decay, $\overline{B}^0 \to D^+\ell^-\bar{\nu}_\ell$ decay and the $\overline{B} \to D\ell^-\bar{\nu}_\ell$ combined fit (ellipse in red). The systematic uncertainties are taken into account.

6 Systematic Uncertainties

Different sources of systematic uncertainties have been estimated and are given in Table 2. We have grouped them into several categories.

Detector-related systematics may arise from differences between the data and simulation of

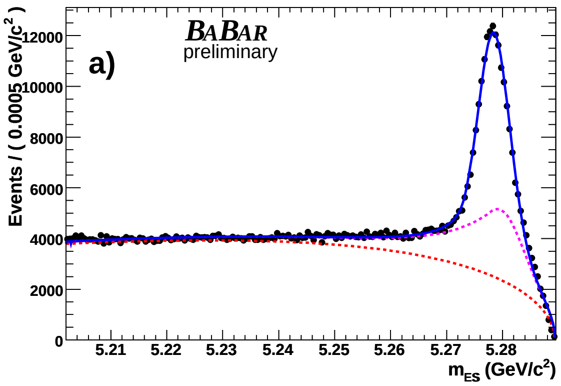

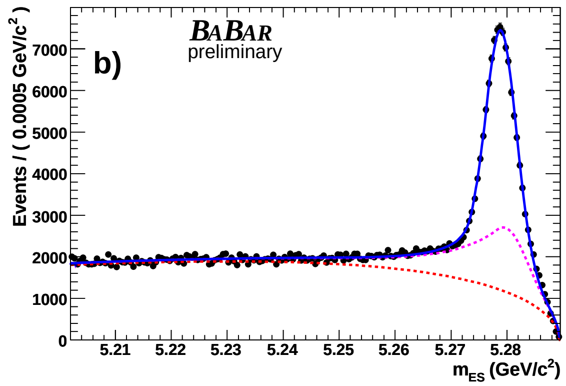

Figure 5: m_{ES} distributions of the a) $B^- \rightarrow X\ell^-\bar{\nu}_\ell$, and b) $\overline{B}^0 \rightarrow X\ell^-\bar{\nu}_\ell$ samples. The data (points with error bars) are compared to the result of the fit (solid line). The dashed lines show the broad-peaking component and the sum of the combinatorial and continuum background.

the track reconstruction and efficiency, particle identification and neutral particle reconstruction. The systematic uncertainty related to the reconstruction of charged tracks is determined by randomly removing a fraction of tracks corresponding to the uncertainty in the track finding efficiency, estimated on $e^+e^- \rightarrow \tau^+\tau^-$ data control samples. The systematic uncertainty due to the reconstruction of neutral particles in the EMC is studied by varying the resolution and efficiency to match those found in data control samples. We estimate the systematic uncertainty due to particle identification by varying the electron and muon identification efficiencies by 2% and 3%, respectively. The misidentification probabilities are varied by 15% for both electrons and muons.

We evaluate the systematic uncertainties associated with the Monte Carlo simulation of the various signal and background processes. The uncertainty arising from radiative corrections is studied by comparing the results using PHOTOS with those obtained with PHOTOS turned off. We take 30% of the difference as a conservative systematic uncertainty. The fraction of B cascade decays in the $\overline{B} \rightarrow X\ell^-\bar{\nu}_\ell$ sample is varied within its uncertainties and the differences in the $\overline{B} \rightarrow X\ell^-\bar{\nu}_\ell$ signal yields are included in the systematic uncertainties. Possible differences in the $B_{\rm tag}$ composition of the MC simulation and data can affect the efficiencies and the cross-feed between charged and neutral B events. To evaluate this effect we assume a conservative 30% systematic uncertainty to the cross-feed fractions and we evaluate the systematic uncertainty by looking at differences in the measured values of $\mathcal{G}(1)|V_{cb}|$ and ρ^2 as we change the cross-feed fractions. We vary the $\overline{B} \rightarrow D^*\ell^-\bar{\nu}_\ell$ form factors within their measured uncertainties [14] and we use an HQET parameterization [23] for $\overline{B} \rightarrow D^{**}\ell^-\bar{\nu}_\ell$. We also vary the $\overline{B} \rightarrow D^{**}\ell^-\bar{\nu}_\ell$ branching fractions within the measured uncertainties [19]. For the $|V_{cb}|$ measurement, we include a contribution due to the uncertainties on the branching fractions of the reconstructed D modes, and on the absolute branching fraction $\mathcal{B}(\overline{B} \rightarrow X\ell^-\bar{\nu}_\ell)$ used for the normalization.

We also evaluate a systematic uncertainty due to differences in the efficiency of the $B_{\rm tag}$ selection in the exclusive selection of $\overline{B} \rightarrow D\ell^-\bar{\nu}_\ell$ decays and the inclusive $\overline{B} \rightarrow X\ell^-\bar{\nu}_\ell$ reconstruction, by using the same $B_{\rm tag}$ candidate selection adopted in the $\overline{B} \rightarrow X\ell^-\bar{\nu}_\ell$ reconstruction also for the $\overline{B} \rightarrow D\ell^-\bar{\nu}_\ell$ decays, and taking the difference in the signal yield, corrected for the difference in the reconstruction efficiency, as a systematic uncertainty.

The systematic uncertainty in the determination of the $\overline{B} \rightarrow X\ell^-\bar{\nu}_\ell$ yield is estimated by using

Table 2: Systematic uncertainties in the measurement of $\mathcal{G}(1)|V_{cb}|$ and ρ^2 for $\overline{B} \to D\ell^-\bar{\nu}_\ell$ decays. We report the relative error (in %) for $\mathcal{G}(1)|V_{cb}|$ and the absolute error on ρ^2.

	Systematic uncertainty on $\lvert V_{cb}\rvert$ and ρ^2					
	$D^0\ell^-\bar{\nu}_\ell$		$D^+\ell^-\bar{\nu}_\ell$		$D\ell^-\bar{\nu}_\ell$	
	$\lvert V_{cb}\rvert$(%)	ρ^2	$\lvert V_{cb}\rvert$(%)	ρ^2	$\lvert V_{cb}\rvert$(%)	ρ^2
Tracking efficiency	0.5	0.008	1.1	0.003	0.7	0.004
Neutral reconstruction	1.	0.003	0.8	0.006	0.9	0.004
Lepton ID	1.0	0.009	0.9	0.009	0.95	0.009
PHOTOS	0.13	0.005	0.10	0.005	0.12	0.005
Cascade $\overline{B} \to X \to \ell^-$ decay background	0.6	-	1.0	-	0.75	-
$\overline{B} - B^-$ cross-feed	0.24	0.003	0.24	0.003	0.24	0.003
$\overline{B} \to D^*\ell^-\bar{\nu}_\ell$ Form factors	0.56	0.008	0.20	0.003	0.38	0.006
$\overline{B} \to D^{**}\ell^-\bar{\nu}_\ell$ Form factors	0.24	0.007	0.34	0.006	0.29	0.007
D branching fractions	1.0	-	1.35	-	1.12	-
$\mathcal{B}(\overline{B} \to D^{**}\ell^-\bar{\nu}_\ell)$	1.18	0.023	0.96	0.011	1.08	0.019
$\mathcal{B}(\overline{B} \to X\ell^-\bar{\nu}_\ell)$	0.95	-	0.95	-	0.85	-
B_{tag} selection	1.1	0.021	1.8	0.036	1.5	0.028
$\overline{B} \to X\ell^-\bar{\nu}_\ell$ yield	0.7	-	1.1	-	0.85	-
$\overline{B} \to D\ell^-\bar{\nu}_\ell$ yield	1.27	0.018	1.06	0.027	1.25	0.020
Total systematic error	3.1	0.04	3.6	0.05	3.3	0.04

an alternative fit method, which is then compared to the result of the nominal m_{ES} fit. We consider the m_{ES} distribution from the data and the combinatorial $B\overline{B}$ continuum and other background components (cascade and hadronic B decays) modeled with distributions taken from the Monte Carlo simulation. We fit the background normalization on data in the m_{ES} sideband region, defined by $m_{ES} < 5.265$ GeV/c^2. The normalization for the continuum background is fixed to the value obtained from off-peak data. The total background contribution is then subtracted from the total number of events in the m_{ES} distribution to extract the $\overline{B} \to X\ell^-\bar{\nu}_\ell$ signal yield. The uncertainty in the determination of the $\overline{B} \to D\ell^-\bar{\nu}_\ell$ yield in the different w intervals is estimated by changing the PDFs used to model the different contributions in the m^2_{miss} distribution, e.g. by replacing the continuum PDFs with the corresponding one obtained from off-peak data.

7 Results

We present a measurement of $\mathcal{G}(1)|V_{cb}|$ and ρ^2 for $\overline{B} \to D\ell^-\bar{\nu}_\ell$. For $B^- \to D^0\ell^-\bar{\nu}_\ell$, we obtain:

$$\begin{aligned} \mathcal{G}(1)|V_{cb}| &= (41.7 \pm 2.1 \pm 1.3) \times 10^{-3} \\ \rho^2 &= 1.14 \pm 0.11 \pm 0.04 \\ \mathcal{B}(B^- \to D^0\ell^-\bar{\nu}_\ell) &= (2.31 \pm 0.08 \pm 0.07)\%, \end{aligned} \tag{6}$$

while for $\overline{B}^0 \to D^+\ell^-\bar{\nu}_\ell$, we obtain:

$$\begin{aligned}\mathcal{G}(1)|V_{cb}| &= (45.6 \pm 3.3 \pm 1.6) \times 10^{-3} \\ \rho^2 &= 1.29 \pm 0.14 \pm 0.05 \\ \mathcal{B}(\overline{B}^0 \to D^+\ell^-\bar{\nu}_\ell) &= (2.23 \pm 0.11 \pm 0.08)\%. \end{aligned} \quad (7)$$

The results of the combined fit are:

$$\begin{aligned}\mathcal{G}(1)|V_{cb}| &= (43.0 \pm 1.9 \pm 1.4) \times 10^{-3} \\ \rho^2 &= 1.20 \pm 0.09 \pm 0.04 \\ \mathcal{B}(\overline{B}^0 \to D^+\ell^-\bar{\nu}_\ell) &= (2.17 \pm 0.06 \pm 0.07)\%. \end{aligned} \quad (8)$$

Using an unquenched lattice calculation [8], corrected by a factor of 1.007 for QED effects, we get

$$|V_{cb}| = (39.8 \pm 1.8 \pm 1.3 \pm 0.9_{FF}) \times 10^{-3} \quad (9)$$

where the third error is due to the theoretical uncertainty in $\mathcal{G}(1)$. The resulting value of $|V_{cb}|$ is fully compatible with the other existing measurements on $\overline{B} \to D\ell^-\bar{\nu}_\ell$, and also with the measurement obtained using $\overline{B} \to D^*\ell^-\bar{\nu}_\ell$. Within the total errors this measurement is also compatible with the inclusive determination of $|V_{cb}| = (41.68 \pm 0.39 \pm 0.58) \times 10^{-3}$ [24].

8 Acknowledgments

We are grateful for the extraordinary contributions of our PEP-II colleagues in achieving the excellent luminosity and machine conditions that have made this work possible. The success of this project also relies critically on the expertise and dedication of the computing organizations that support *BABAR*. The collaborating institutions wish to thank SLAC for its support and the kind hospitality extended to them. This work is supported by the US Department of Energy and National Science Foundation, the Natural Sciences and Engineering Research Council (Canada), the Commissariat à l'Energie Atomique and Institut National de Physique Nucléaire et de Physique des Particules (France), the Bundesministerium für Bildung und Forschung and Deutsche Forschungsgemeinschaft (Germany), the Istituto Nazionale di Fisica Nucleare (Italy), the Foundation for Fundamental Research on Matter (The Netherlands), the Research Council of Norway, the Ministry of Education and Science of the Russian Federation, Ministerio de Educación y Ciencia (Spain), and the Science and Technology Facilities Council (United Kingdom). Individuals have received support from the Marie-Curie IEF program (European Union) and the A. P. Sloan Foundation.

References

[1] M. Kobayashi and T. Maskawa, Prog. Theor. Phys. **49**, 652 (1973).

[2] N. Isgur and M. B. Wise, Phys. Rev. Lett. **66**, 1130 (1991).

[3] K. Abe *et al.* (Belle *Coll.*), Phys. Lett. B **526**, 258 (2002).

[4] J. Bartelet *et al.* (CLEO *Coll.*), Phys. Rev. Lett. **82**, 3746 (1999).

[5] D. Buskulic *et al.* (ALEPH *Coll.*), Phys. Lett. B **395**, 373 (1997).

[6] Charge conjugate states and transitions are always implied, unless explicitely stated otherwise.

[7] N. Isgur and M. B. Wise, Phys. Lett. B **232**, 113 (1989); and ibid. **237**, 527 (1990).

[8] M. Okamoto *et al.* Nucl. Phys. (Proc. Supp.) **140**, 461 (2005).

[9] I. Caprini, M. Neubert, Phys. Lett. B **380**, 376 (1996), and C. G. Boyd, B. Grinstein, R. F. Lebed, Phys. Rev. D **56**, 6895 (1997).

[10] I. Caprini, L. Lellouch, M. Neubert, Nucl. Phys. B **530**, 153 (1998).

[11] B. Aubert *et al.* (*BABAR* Collaboration), Nucl. Inst. Meth. A **479**, 1 (2002).

[12] S. Agostinelli *et al.*, Nucl. Inst. Meth. A **506**, 250 (2003).

[13] D. Scora and N. Isgur, Phys. Rev. D **52**, 2783 (1995), and N. Isgur *et al.*, Phys. Rev. D **39**, 799 (1989).

[14] B. Aubert *et al.* (*BABAR* Collaboration), Phys. Rev. D **77**, 032002 (2008).

[15] J. L. Goity and W. Roberts, Phys. Rev. D **51**, 3459 (1995).

[16] E. Barberio and Z. Was, Comp. Phys. Commun. **79**, 291 (1994).

[17] H. Albrecht *et al.* (ARGUS Collaboration), "Exclusive semileptonic decays of B mesons to D mesons", DESY-92-029 (1992).

[18] R. J. Barlow and C. Beeston, Comput. Phys. Commun. **77**, 219 (1993).

[19] W. -M. Yao *et al.* (Particle Data Group), J. Phys. G **33**, 1 (2006) and 2007 partial update for 2008.

[20] B. Aubert *et al.* (*BABAR* Collaboration), Phys. Rev. D **74**, 091105 (2006).

[21] H. Albrecht *et al.* (ARGUS Collaboration), Z. Phys. C **48**, 543 (1990).

[22] M. J. Oreglia, SLAC-236 (1980); J. E. Gaiser, SLAC-255 (1982); T. Skwarnicki, DESY F31-86-02 (1986).

[23] A. K. Leibovich, Z. Ligeti, I. W. Stewart and M. B. Wise, Phys. Rev. D **57**, 308 (1998).

[24] Heavy Flavor Averaging Group, http://www.slac.stanford.edu/xorg/hfag/semi/pdg08/home.shtml.